

## Study on the Corrosion Inhibition Effect of 2,3-Dimercapto-1-propanol on Copper in 0.5mol/L H<sub>2</sub>SO<sub>4</sub> Solution

Denglin Fu<sup>1</sup>, Bochuan Tan<sup>1</sup>, Lansu Lu<sup>1</sup>, Xin Qin<sup>2</sup>, Shijin Chen<sup>3</sup>, Wei He<sup>4</sup>, Jida Chen<sup>1,\*</sup>

<sup>1</sup> School of Chemistry and Chemical Engineering, Chongqing University, Chongqing 400044, P R China

<sup>2</sup> Jiangsu Bomin electronics Ltd, Yancheng, Jiangsu 224100, P.R. China

<sup>3</sup> Bomin electronics Ltd, Meizhou, Guangdong 514021, P.R. China

<sup>4</sup> Materials and Energy Institute, University of Electronic Science and Technology of China (UESTC), Chengdu, Sichuan 610054, P.R. China

\*E-mail: [chencqu@cqu.edu.cn](mailto:chencqu@cqu.edu.cn)

Received: 5 April 2018 / Accepted: 29 May 2018 / Published: 5 August 2018

---

In this paper, the inhibition performance of 2,3-Dimercapto-1-propanol (DIP) in 0.5 M sulfuric acid were studied by polarization curves, impedance spectroscopy, scanning electron microscopy, atomic force microscopy and theoretical calculations. The results of electrochemical experiments manifest that DIP is a cathode corrosion inhibitor that can produce a compact protective membrane on the surface of copper, which can effectively reducing the corrosion current density. Field emission scanning electron microscope (FE-SEM) and atomic force microscopy (AFM) certificated that a conservational membrane was produced on the surface of the inhibited sample. In addition, the adsorption of the inhibitor was found to be consistent with the Langmuir isotherm. Molecular dynamics simulations and quantum chemical calculations were applied to elucidate the adsorption mode of inhibitor molecules on copper surfaces.

---

**Keywords:** Electrochemical test, Quantum chemical calculations, Corrosion inhibitor, copper

### 1. INTRODUCTION

Copper is extensively used in different, such as defense industry, shipbuilding industry, and electronics trade because of its excellent electrical conductivity, mechanical properties and thermal conductivity. Among them, the electronic industry is the most widely used. In the electronic production process, the production of printed circuit boards is a crucial step. In the production process of printed circuit boards, sulfuric acid is usually used to pickle the copper substrates to achieve the

purpose of cleaning the surface. However, in the pickling process, sulfuric acid can also corrode the copper surface, which will not only affect the subsequent production process, but also cause consumption of sulfuric acid and waste of metal resources. Furthermore, a lot of commonly applied corrosion inhibitors are harmful to the human body and other living creature, some corrosion inhibitors are difficult to degrade due to their complex molecular structure and have great environmental hazards. Hence, the corrosion of copper in sulfuric acid solution and corrosion inhibitors have aroused attention from a number of researchers [1-4].

Organics are the most important class of copper corrosion inhibitors [1-8]. However, with the development of the concept of environmental protection, some conventional corrosion inhibitors have been gradually eliminated due to their toxicity. Green corrosion inhibitors have become a research hotspot due to their environmental friendliness and non-toxicity.

2,3-Dimercapto-1-propanol as an antidote can relieve poisoning of all arsenic poisons and heavy metals (such as gold, antimony, cadmium, tellurium, mercury, etc.) [9]. Low-dose DIP has less pollution to the environment, no harm to the human body. Therefore, it is an environment-friendly corrosion inhibitor. The intent of this job is to research the rejection capability of DIP on copper corrosion in 0.5M sulfuric acid solutions at 298 K. Scanning electron microscopy (SEM), atomic force microscopy (AFM), electrochemical impedance spectroscopy (EIS), electrochemical polarization curves, were applied to study the inhibiting performance of copper from DIP in 0.5 M H<sub>2</sub>SO<sub>4</sub> solutions. In addition, the adsorption mechanism and active sites of DIP on copper surface were studied by theoretical calculation.

## 2. EXPERIMENTAL

### 2.1 Materials and sample preparation

2,3-Dimercapto-1-propanol (Ron's reagent) is the inhibitor, and its molecular constitution is displayed in Figure 1. The corrosion solution is made up of 98% concentrated sulfuric acid (analytical grade) and ultrapure water at a concentration of 0.5 M. The concentration of 2,3-Dimercapto-1-propanol inhibitor ranges from 0.1 mM to 5 mM and is compared with a blank solution containing no inhibitor.

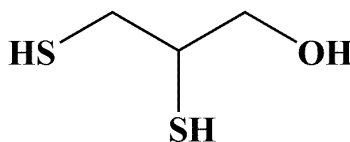


**Figure 1.** Chemical structure of the Dimercaptopropanol.

### 2.2. Electrochemical measurements

In this article, the electrochemical experiment was conducted by the CHI604D electrochemical station using the classical three-electrode method. The working electrode is a copper sheet sealed with epoxy resin, the reference electrode was a saturated calomel electrode (SCE), and the auxiliary electrode is a platinum electrode with a size of 2 cm x 2 cm, all test potentials are relative to the reference electrode. Before the electrochemical experiment was started, the copper working electrode was soaked in the OCP (open circuit potential) test solution for 1 hour to reach a steady-state. In the electrochemical impedance spectroscopy (EIS) measurement, a sine-wave interference signal was used. The amplitude of the sine wave was 10 mV, and the range of scanning frequency was from  $10^5$  Hz to  $10^{-2}$  Hz. Impedance data processing using Zsimpwin software, and the structure of the equivalent circuit and the parameters of each component are analyzed. The scanning rate of the potentiodynamic polarization curve was 1 mV/s and the sweep scope was -250 to 250 mV (vs. OCP), which was fitted linearly in the Tafel region to obtain electrochemical corrosion parameters. In order to obtain an approving reproducibility, experiments were performed 3 times under the same conditions.

### 2.3 Corrosion morphology analysis

Copper samples (0.5 cm x 0.5 cm x 0.5 cm) were soaked in a 0.5 M sulfuric acid solution without and with DIP for 8 h at a temperature of 298 K. Under high vacuum, a field emission scanning electron microscope (FE-SEM, JEOL-JSM-7800F, JEOL Ltd., Japan) was used to record the surface morphology of the copper sample. In addition, the AFM (atomic force microscopy, Asylum Research, America) test is performed under the same conditions by applying tapping method.

### 2.4 Quantum chemical calculations

Recently, quantum chemical calculations are commonly used to define molecular structure and clarify electronic structure and active sites [10-12]. Quantum chemistry calculations can explain the results obtained during the experiment from the molecular level [13]. The initial configuration of the calculated molecule was constructed by the Gaussview program, then use the DMol3 module of Material Studio 8.0 to perform quantum chemistry calculations of DIP molecules, and use density functional theory (DFT) to optimize the geometry of the studied molecules [14, 15]. Corresponding quantum chemical parameters were also obtained, for example, the molecular energy of the highest occupied orbit  $E_{\text{HOMO}}$  and the lowest energy empty orbit  $E_{\text{LUMO}}$ , the dipolar moment  $\mu$  and the energy disparity  $\Delta E$  ( $\Delta E = E_{\text{LUMO}} - E_{\text{HOMO}}$ ).

For better understanding the adsorption behavior of DIP on copper surfaces, molecular dynamics simulations of the interaction of DIP on the Cu (111) surface under vacuum conditions using Accelrys Inc. forcite module were performed using COMPASS with periodic boundary conditions. In the force field, the interaction between the copper surface (111) and DIP is presumed to be in an emulation box of size 2.2 x 2.6 x 4.3 nm<sup>3</sup>. Simulation of 300 molecules of water and one DIP molecule inhibitor interacts freely with the copper facade, and Cu atoms of all six layers maintained "congealed" by setting their location. During the molecular dynamics imitation, the dominate requirements are the

emulation temperature of 298K and the NVT standard unit, the period increment is 1fs, and the emulation time is 500 ps [1,2].

### 3. RESULTS AND DISCUSSION

#### 3.1. Potentiodynamic polarization curves

The polarization curves is displayed in Figure 2 for copper in 0.5 M sulfuric acid solution without and with various concentrations of DIP at 298 K. By extrapolating the Tafel linearity area, the electrochemical parameters of the copper electrode in a 0.5M sulfuric acid solution with non-existence and existence of various contents of DIP were obtained, including cathode and anode Tafel slopes ( $\beta_c, \beta_a$ ), corrosion potential ( $E_{corr}$ ), corrosion current density ( $I_{corr}$ ) and corrosion suppression ability ( $\eta$ ). These parameters are counted and showed in Table 1, where  $\eta$  is calculated as follow;

$$\eta(\%) = \frac{I_{corr,0} - I_{corr}}{I_{corr,0}} \times 100$$

Where  $I_{corr}$  is the current density of the protected copper coupon and  $I_{corr,0}$  is the current density of the unprotected copper coupon.

From Figure 2 can be concluded that with the DIP adding into the 0.5M sulfuric acid solution, the corrosion current density is significantly reduced, and as the concentration increases, the polarization curves shift obviously to the negative potentials. Furthermore, the inhibitory capability of DIP on the cathode is significantly better than that on the anode. This signifies that DIP molecules are mainly absorbed on the copper face, and primarily limits the metastasis of oxygen from bulk solution to the cathode position of copper-based [2].

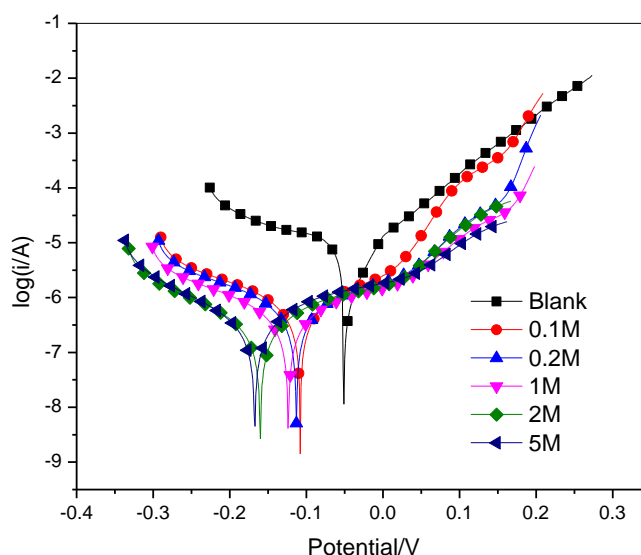


**Figure 2.** Polarization curves for copper in 0.5 M  $H_2SO_4$  in the absence and presence of different concentrations of DIP at 298 K.

Table 1 shows that with the increase of the DIP concentration, the cathode Tafel slope has undergone a great change, it can be explained that DIP molecules form a dense molecular membrane on the surface of copper, hence the corrosion of copper by  $H_2SO_4$  is inhibited, and the inhibitor mainly controls the cathodic reaction [16-19]. What's more, with concentration of DIP increases, the corrosion current density gradually decreases, but the corrosion inhibition effect  $\eta$  gradually enlarges with the increase in concentration. This is because as the concentration of DIP increases, the copper surface is covered by more and more DIP molecules, generating a dense molecular membrane, and the corrosion inhibition effect is getting better and better [16]. Besides, compared with the corrosion potential of the blank solution, the displacement of the corrosion potential after adding DIP is greater than 85mV, so DIP is a cathode or anode type corrosion inhibitor [20-22]. On the other hand, compared with the blank experiment, the  $E_{corr}$  value was more negative in the inhibitory system, indicating that DIP is mainly a cathodic inhibitor [23].

**Table 1.** Electrochemical parameters for copper in 0.5 M  $H_2SO_4$  in the absence and presence of different concentrations of DIP at 298 K.

C(mM)	$E_{corr}$ (mV/SCE)	$I_{corr}$ ( $\mu A\ cm^{-2}$ )	$\beta_c$ (mV $dec^{-1}$ )	$\beta_a$ (mV $dec^{-1}$ )	$\eta$ (%)
Blank	-51	10.45	-259.81	219.30	—
DIP					
0.1	-113	0.937	-194.78	243.01	91.03
0.5	-115	0.84	-189.97	237.19	91.96
1	-127	0.72	-186.81	255.43	93.11
2	-167	0.44	-139.37	225.02	95.79
5	-181	0.28	-114.42	223.71	97.32

### 3.2. Electrochemical impedance spectroscopy

For the purpose to obtain more information of DIP in the inhibition process, EIS measurements were carried out on copper electrode. Figure 3 is a Nyquist diagram showing the electrochemical impedance spectra of copper in 0.5 M  $H_2SO_4$  solution with non-existence and existence various contents of inhibitors.

Figure 3 exhibits that the impedance curve is linear at low frequency and semicircular at high frequent. High frequency relates to the capacitive reactance arc, which is affiliated with the electric double layer capacitance and charge transfer resistance ( $R_{ct}$ ). Low frequency corresponds to the Warburg impedance, the low-frequency line means that copper erosion in 0.5 M  $H_2SO_4$  solution is controlled by diffusion, this may be owing to the soluble corrosion products and transport of corrosive ions or soluble oxygen to the face of copper at the solution/metal interface [24, 25]. From Fig. 3 and its inset, we were able to conclude that the shape and size of the high-frequency capacitance arc increases with the increasing of DIP concentration, which indicates that DIP forms a dense film at the copper surface and effectively inhibit charge transfer between copper and sulfuric acid [26-28]. Besides a second semi-circle of the capacitor emerges at the mid and low frequency, this is owing to surface

roughness, surface inhomogeneity and the existence of two diverse procedures that actually own the identical relaxation time [28].

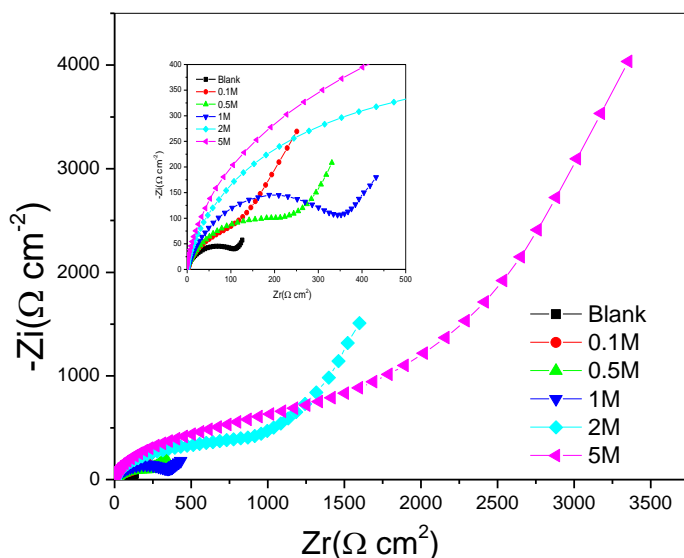


**Figure 3.** Nyquist plots recorded for the copper electrode in 0.5 M H<sub>2</sub>SO<sub>4</sub> solution containing different concentrations of DIP at 298 K.

Figure 4 exhibits the Bode diagram of the tested electrochemical impedance. From Figure 4(a), as the DIP concentration increases, the impedance grows dramatically over the entire frequency purview, which manifests that an obvious increase in the corrosion resistance of copper [29,30]. In addition, from Figure 4 (b), the frequency domain of the maximum phase angle also gradually increased, demonstrating that DIP can better adsorb on the copper face to restrain erosion [2].

The equivalent circuitry exhibits in Figure 5 is used to fit the corresponding impedance parameters, the obtained electrochemical data is exhibited in Table 2. In the equivalent circuitry components, CPE represents a constant phase angle element, W stands for Warburg impedance, R<sub>s</sub> is solution resistance, CPE<sub>f</sub> and R<sub>f</sub> are the erosion products film capacitance and film resistance of the copper surface, CPE<sub>dl</sub> is a double layer capacitor between the copper surface and the solution and R<sub>ct</sub> is the charge transfer resistor. The impedance of CPE is calculated as following formula [31].

$$Z_{CPE} = \frac{1}{Y_0(j\omega)^n}$$

where  $\omega$  represents the angular frequency,  $j$  represents the imaginary root and  $Y_0$  represents the value of CPE,  $n$  is the dispersion effect index, the constant phase angle element CPE can be capacitance ( $n = 1$ ), inductive reactance ( $n = -1$ ), Warburg impedance ( $n = 0.5$ ) and resistance ( $n = 0$ ). When the value of  $n$  is between 0.5 and 1, CPE is the distribution of the dielectric relaxation time in the frequency space [32].

The relevant resistance parameters are exhibited in Table2. Calculation of the suppression efficiency of copper in 0.5M H<sub>2</sub>SO<sub>4</sub> solution with various contents of DIP is derived from the polarized resistance Rp (Rp is the sum of R<sub>f</sub> and R<sub>ct</sub>);

$$\eta(\%) = \frac{R_p - R_{p,0}}{R_p} \times 100$$

Where  $R_{p,0}$  represents the summation of the resistance and charge transfer resistance of the copper film in a 0.5 M sulfuric acid solution with non-existence of DIP,  $R_p$  represents the summation of charge transfer resistor and membrane resistor.

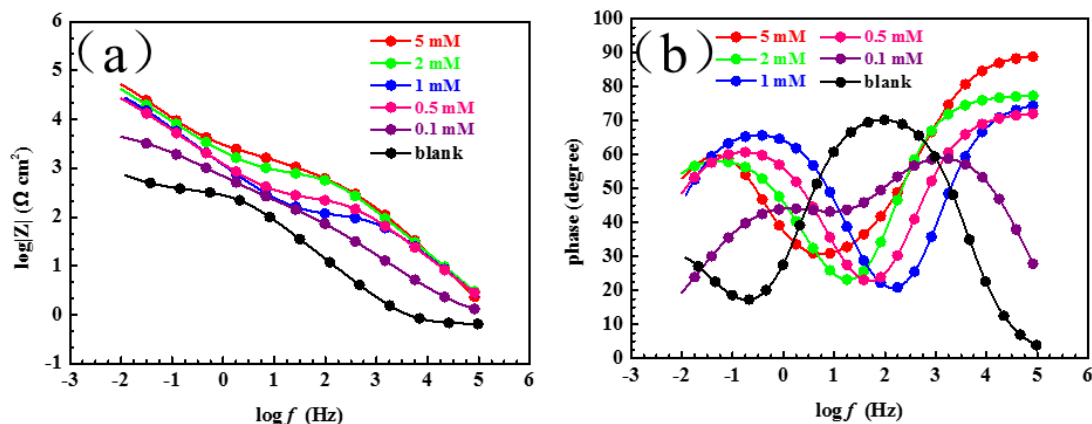


**Figure 4.** Bode graphs for copper in 0.5 M H<sub>2</sub>SO<sub>4</sub> without and with various concentrations of DIP at 298 K; (a) impedance plot of DIP (b) phase angle plot

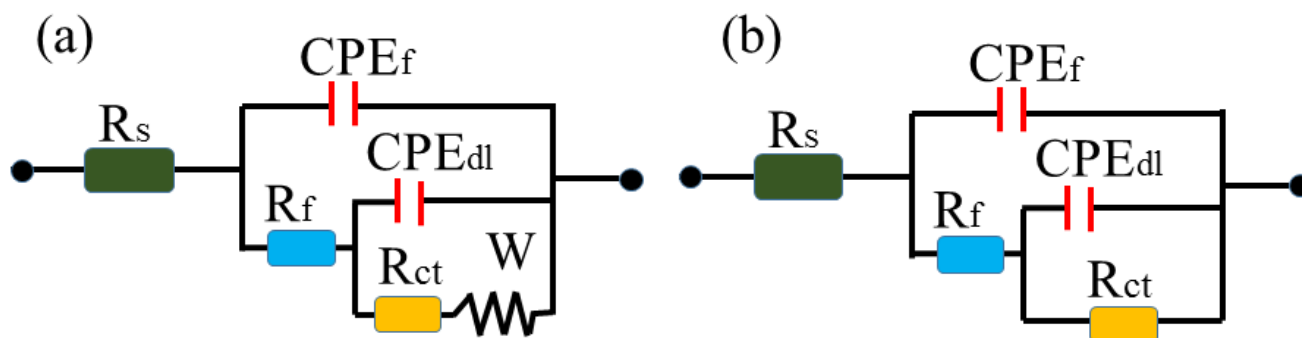


**Figure 5.** Electrochemical equivalent circuits applied to fit the impedance relevant data.

From Table 2, we can conclude that with the concentration of DIP increases, corrosion inhibition efficiency and the value of charge transfer resistance ( $R_{ct}$ ) increase, which suggests that DIP has a good corrosion suppression effect on copper in 0.5 M H<sub>2</sub>SO<sub>4</sub> solution. On the contrary, the  $C_{dl}$  and  $C_f$  values reduce with the addition of more DIP inhibitors, which is considered to be caused by the absorption of corrosion inhibitors on the surface of electrode [33]. It can be explained as follows;

$$C_{dl} = \frac{\epsilon^0 \epsilon}{d} S$$

Where,  $\epsilon$  is the partial dielectric coefficient,  $\epsilon^0$  is the dielectric constant of the air,  $d$  is double layer thickness, and  $S$  is the superficial area of the copper electrode. Since the sorption of the corrosion inhibitor is a procedure that replaces water molecules, the permittivity at the interface between the solution and the copper decreases or the thickness of the bilayer increases, resulting in a

reduce in  $C_{dl}$  [34]. The reduction of  $C_f$  can be explicated by a decrease of the exposed superficial area of the electrode at high inhibitor contents [14]. Moreover, the corrosion suppression ability obtained by electrochemical impedance spectroscopy agrees well with the polarization curve.

**Table 2.** Impedance parameters of copper in 0.5 M  $H_2SO_4$  solution in the absence and presence of DIP at 298 K.

$C$ (mM)	$R_f$ ( $k\Omega\text{ cm}^2$ )	$R_{ct}$ ( $k\Omega\text{ cm}^2$ )	$R_p$ ( $k\Omega\text{ cm}^2$ )	$C_f$ ( $\mu\text{F cm}^{-2}$ )	$n_1$	$C_{dl}$ ( $\mu\text{F cm}^{-2}$ )	$n_2$	$W$ ( $\times 10^{-2}\Omega\text{ cm}^2\text{ s}^{1/2}$ )	$\eta$ (%)
Blank	0.01	0.40	0.41	43.2	0.93	52.0	0.43	1.31	—
0.1	0.02	6.19	6.21	26.1	0.73	31.4	0.56	—	93.3
0.5	0.07	38.6	38.76	19.5	0.78	23.9	0.69	—	98.9
1	0.12	42.4	42.52	21.3	0.84	19.6	0.77	—	99.0
2	0.35	66.1	66.45	23.6	0.86	13.8	0.71	—	99.3
5	0.31	71.5	71.81	17.5	0.56	10.3	0.96	—	99.4

### 3.3. Scanning electron microscopic study

In the interest of further study the corrosion inhibition result of DIP, the erosion morphology of the copper sample at 298 K after etched for 8 h in  $H_2SO_4$  solution without and with DIP was measured by SEM. As the Figure 6(a) displays, the corrosion of the copper surface by  $H_2SO_4$  in the absence of DIP is very severe, whereas Figure 6 (b) shows that with the addition of 5mM DIP in the sulfuric acid solution, the copper face is flat and smooth, which further certifying that the good erosion suppression of DIP for copper in sulfuric acid solution.

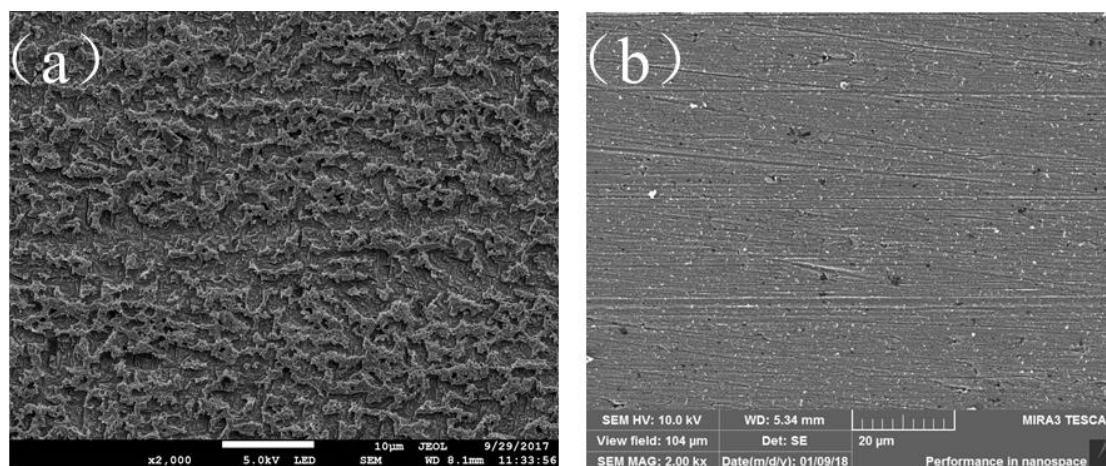


**Figure 6.** The copper surface dipped in 0.5 M  $H_2SO_4$  solution without DIP (a) and with 5 mM DIP (b) of SEM for 8 h at 298 K.

### 3.4 AFM observation

To further study the adsorption process of inhibitors at the solution/metal interface, we used the atomic force microscope to study the 3D map and height profiles of copper in the 0.5 M  $\text{H}_2\text{SO}_4$  solution without and with 5 mM DIP for 8 h at 298 K. Three-dimensional (3D) topography are displayed in Figures 7(a) and 7(c), it can be clearly seen from the 3D diagram that the copper surface without DIP is heavily corroded by  $\text{H}_2\text{SO}_4$ , and the copper surface is very rough with an average roughness of 62.564 nm. However, the copper surface after adding 5 mM DIP is relatively flat and smooth, and its average roughness is reduced to 18.144 nm. This manifests that DIP can form a dense conservatory membrane on the copper face, thereby effectively inhibiting the copper erosion in  $\text{H}_2\text{SO}_4$  solution. Obviously, the results obtained by atomic force microscopy agree well with the results obtained by SEM images.

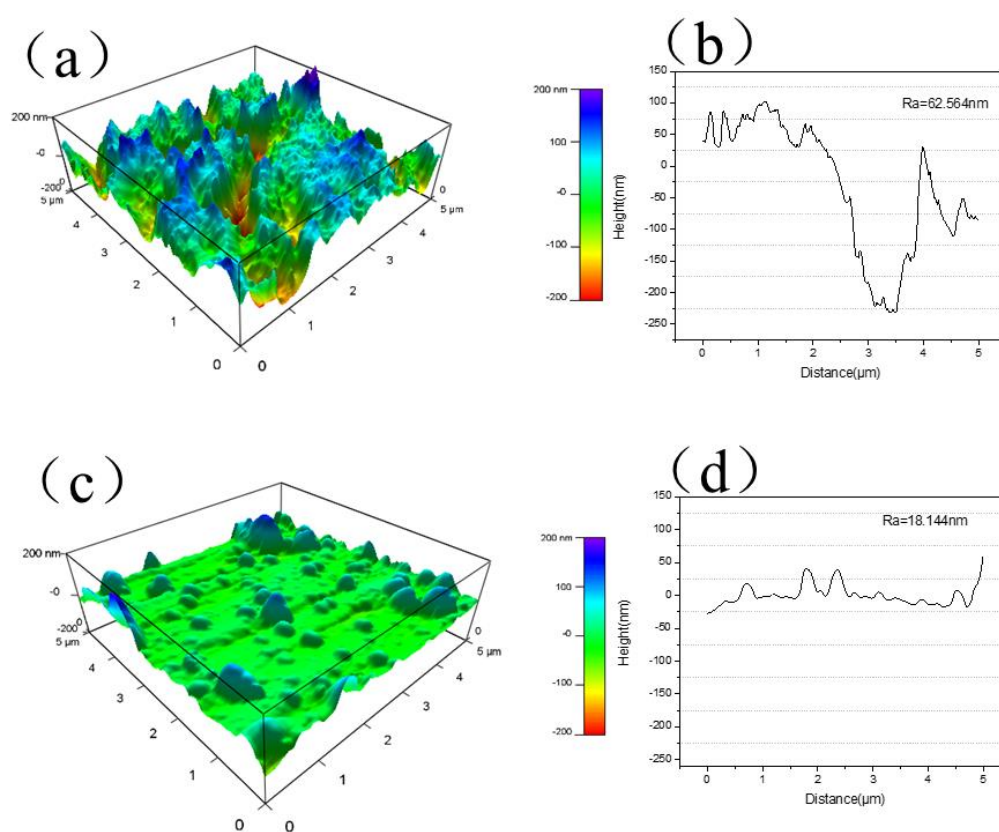


**Figure 7.** The three-dimensional AFM images and corresponding height profile graphs of (a, c) corroded copper, (b, d) protected copper by DIP in 0.5 M  $\text{H}_2\text{SO}_4$  solution for 8 h at 298 K.

### 3.5 Quantum chemical research

For further research the adsorption of DIP on copper face and research its impact on corrosion inhibition mechanisms, the geometric structure of DIP was optimized by quantum chemical methods. At the same time, Table 3 displays the calculation results of the corresponding quantum chemical parameters such as  $\Delta E$ ,  $\mu$ ,  $E_{\text{HOMO}}$ , and  $E_{\text{LUMO}}$ , and Figure 8 exhibits the electron cloud distribution of LUMO and HOMO.

As Figure 8 displays, the electron cloud distributions of LUMO and HOMO are majorly concentrated on two thiol groups, indicating that the two S atoms on the thiol group are the DIP active adsorption centers on the copper surface [35, 19]. The frontier orbit theory of quantum chemistry holds that the energy  $E_{\text{HOMO}}$ , which is the highest occupied orbital of molecules, is a mensuration of the capability of the molecule to give electrons. The higher the  $E_{\text{HOMO}}$ , the stronger the ability to provide electrons, and the stronger the ability to form coordination bonds. The energy of the molecule's lowest empty orbit is dependent on the electron affinity of the molecule. The lower its value, the stronger the ability of the molecule to get electrons [36]. The  $\Delta E$  is an important measure of molecular stability, the larger the value, the more stable the molecule [37-39]. Previous reports pointed out that the higher value of the  $\mu$  and the lower value of the  $\Delta E$ , there will be the higher corrosion inhibition efficiency[35,40-42], which means that high dipole moment values and low  $\Delta E$  values can enhance the adsorption of inhibitors on copper surfaces[43,44]. The data in Table 3 shows that both the  $E_{\text{HOMO}}$  and  $E_{\text{LUMO}}$  values are low, demonstrating that DIP is more receptive to electronics than electron loss, DIP has a higher  $\mu$ (3.6029Debye ( $12.018 \times 10^{-30}\text{Cm}$ )) value than  $\text{H}_2\text{O}$ ( $\mu= 6.23 \times 10^{-30}\text{Cm}$ )[43], which may help DIP adsorbed on the copper surface to displace water molecules.

**Table 3.** Related quantum chemical parameters of the DIP.

$E_{\text{HOMO}}(\text{eV})$	$E_{\text{LUMO}}(\text{eV})$	$\Delta E(\text{eV})$	$\mu(\text{D})$
-5.335	-0.689	4.646	3.6029

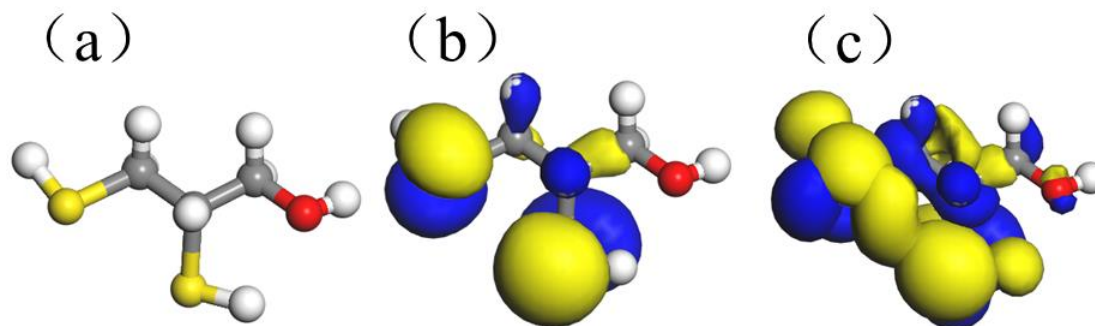


**Figure 8.** Optimized structure (a) and HOMO (b) and LUMO (c) frontier orbital density distribution of DIP.

### 3.6 Molecular dynamics simulations

For further understand the adsorption behavior of DIP on copper surfaces, molecular kinetics simulations were used to discuss the sorption theory of these DIP molecules on the copper face. Figures 9 (a) and (b) show a side view and a top view of the optimal equilibrium of the DIP on a copper (111) surface. It can be seen that due to the interaction between the two S atoms of DIP and  $\text{Cu}^+$  or  $\text{Cu}^{2+}$  to form a coordination bond, DIP molecules tend to absorb on the copper face in a closely parallel pattern [16]. In addition, the adsorption interaction energy ( $E_{\text{interact}}$ ) between the copper surface and DIP is calculated by the following formula [45];

$$E_{\text{interact}} = E_{\text{tot}} - (E_{\text{subs}} + E_{\text{inh}})$$

Where  $E_{\text{subs}}$  represents the energy of H<sub>2</sub>O molecules and copper substrates,  $E_{\text{tot}}$  represents the total energy of the entire configuration,  $E_{\text{inh}}$  is the energy of DIP. The interaction energy value  $E_{\text{interact}}$  calculated from the above formula is  $-215.45$  kJ/mol, which demonstrating that the DIP molecule can powerfully absorb on copper surface.

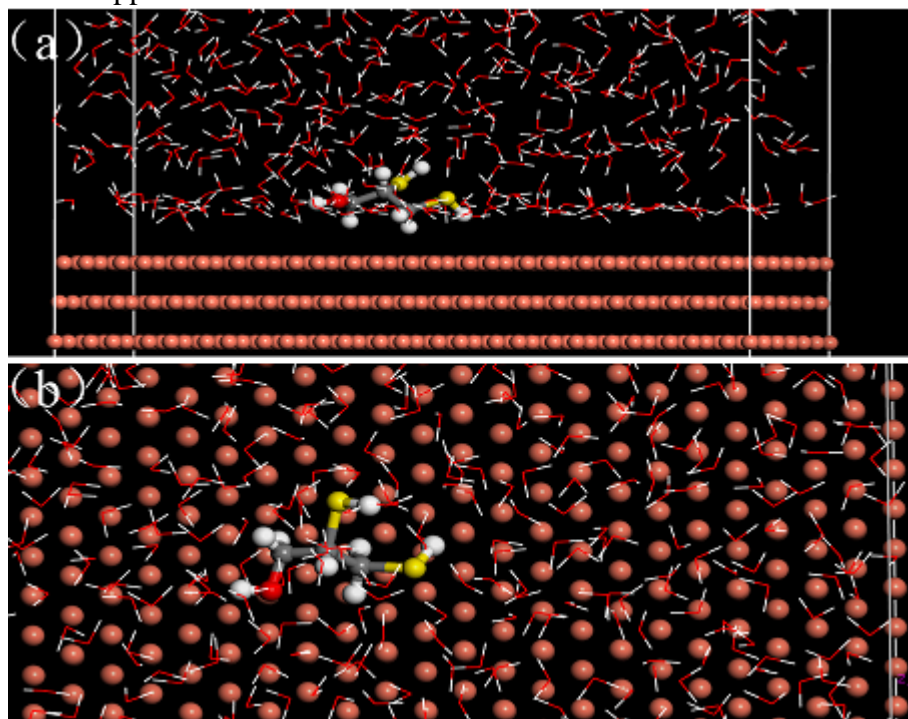


**Figure 9.** Equilibrium configurations for the adsorption of DIP on Cu (111) surface: (a) the side views (b) the top views.

### 3.7 Adsorption isotherm analyze

Due to the organic corrosion inhibitors mainly play a role in corrosion inhibition by conglutinating on metal surface, the study of sorption isothermal equations of corrosion inhibitors on metal surface helps to understand the adsorption behavior and erosion inhibition mechanism of corrosion inhibitor. Using the electrochemical polarization data in Table 1, an adsorption isotherm model for DIP on copper surfaces was fitted. The results showed that Langmuir adsorption isotherm equation can well describe the adsorption behavior of DIP on copper surface. The results are shown in Figure 10, the fitted adsorption parameters and calculated  $\Delta G_{\text{ads}}$  values are also listed in Figure 10. This isotherm calculated as follow [46-48];

$$\frac{\theta}{1-\theta} = K_{\text{ads}} C$$

Where,  $C$  is defined as the consistence of DIP,  $\theta$  (coverage of degree) is defined as  $\eta$  (%),  $K_{\text{ads}}$  is the equipoise constant of adsorption procedure of corrosion inhibitors.

The good linearity and the large correlation coefficient  $R$  in Figure 10 illustrate the reliability of the fitting result. Moreover it can be seen from Figure 10 that both the slope of the line and the

linear regression coefficient (R) are approach to 1, which indicates that the absorption of DIP on copper face satisfies the Langmuir isotherm equation and exhibits single layer absorption characteristics [49]. The following formula is the calculation of the normal absorption free energy ( $\Delta G_{ads}^0$ ) [46, 47, 50];

$$K_{ads} = \frac{1}{55.5} \exp\left(-\frac{\Delta G_{ads}^0}{RT}\right)$$

Where T is the absolute temperature, R represents the molar gas constant and 55.5 stands for the molar concentration of water in the solution.

It is generally considered that when the energy value is larger than  $-20 \text{ kJ mol}^{-1}$ , it belongs to physisorption, which mainly involved in the static electronic effect between the electrified metal surface and the electrified molecules; when the energy value is smaller than  $-40 \text{ kJ mol}^{-1}$ , it belongs to chemisorption, which is due to electronic sharing or charge-shift from the DIP molecules to the copper face to produce a covalent linkage [51-54]. In this article, the criterion free energy of adsorption ( $\Delta G_{ads}^0$ ) calculated from the above formula is  $-35.76 \text{ kJ/mol}$ , which suggests that the sorption of DIP touches upon both physisorption and chemisorption. However, the standard adsorption free energy ( $\Delta G_{ads}^0$ ) value is approaching to  $-40 \text{ kJ/mol}$ , so this means that because of the covalent linkage generated by charge sharing or transfer, DIP is majorly chemisorbed on the copper surface [55-57]. Besides, the larger value of  $K_{ads}$  illustrates that DIP can adsorb more strongly on the copper surface [58,59].

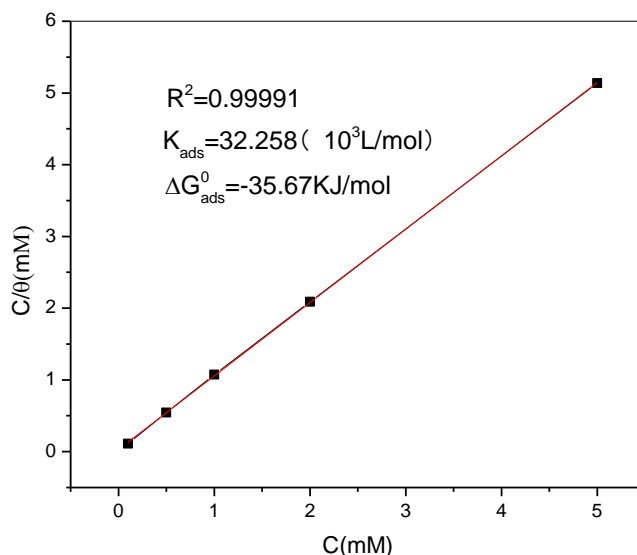


**Figure 10.** Langmuir isotherm plots for copper in 0.5M  $\text{H}_2\text{SO}_4$  solution including diverse concentrations of DIP at 298 K.

#### 4. CONCLUSION

(1) The results of electrochemical experiments revealed that DIP is a cathodic corrosion inhibitor that can adsorb a dense conservational membrane on the external of copper and effectively suppress the erosion of  $\text{H}_2\text{SO}_4$  solution on the copper face.

(2) Atomic force microscopy (AFM) and scanning electron microscopy (SEM) images demonstrate that the surface of the copper sample with DIP in the 0.5 M  $\text{H}_2\text{SO}_4$  solution is smoother than the copper surface without DIP, owing to the sorption of DIP on the copper surface.

(3) Theoretical calculations shows that due to the interaction between the two S atoms of DIP and  $\text{Cu}^+$  or  $\text{Cu}^{2+}$  to form a coordination bond, DIP molecules tend to sorb on the Cu surface in a closely parallel way.

(4) A good linear relationship between the Langmuir isotherm equation and experimental data was found by fitting the isothermal equation. In addition, these DIP molecules are primarily chemisorbed on the copper appearance owing to charge transfer or sharing of formed covalent bonds.

#### ACKNOWLEDGMENTS

This study was completed with the support of the projects of “Sail Plan for Talents Development” of Guangdong Province China (No. 2015YT02D025) and Science and Technology Planning of Guangdong Province (No. 2015B090901032).

#### References

1. B. Tan, S. Zhang, Y. Qiang, *Journal of Molecular Liquids*, 248(2017)902.
2. Y. Qiang, S. Zhang, L. Guo, X. Zheng, B. Xiang, S. Chen, *Corrosion Science*, 119 (2017) 68.
3. G. Quartarone, M. Battilana, L. Bonaldo, *Corrosion Science*, 50(2008)3467.
4. M. A. Elmorsi, A. M. Hassanein, *Corrosion Science*. 41(1999)2337.
5. Marija Petrovic Mihajlovic, Milan B. Radovanovic, Žaklina Z. Tasic and M.M. Antonijevic, *Journal of Molecular Liquids*, 225(2016)127.
6. H. Tian, Y. F. Cheng, W. Li, *Corrosion Science*, 100(2015)341.
7. X. H. Zhang, Q. Q. Liao, K. B. Nie, *Corrosion Science*, 93(2015)201.
8. S. Hong, W. Chen, Y. Zhang, *Corrosion Science*, 66(2013)308.
9. W. T. Longcope, J. A. L. Jr, E. Calkins, *Journal of Clinical Investigation*, 25(1946)557.
10. G. Gece, *Corrosion Science*, 50(2008)2981.
11. N. A. Wazzan, *Journal of Industrial & Engineering Chemistry*, 26(2015)291.
12. H. Mi, G. Xiao, X. Chen, *Computational & Theoretical Chemistry*, 1072(2015)7.
13. I. Ahamad, R. Prasad, M. A. Quraishi, *Corrosion Science*, 52(2010)3033.
14. Y. Qiang, S. Zhang, S. Xu, *Rsc Advances*, 5(2015)63866.
15. L. Guo, S. Zhu, S. Zhang, Q. He, W. Li, *Corrosion Science*, 87 (2014) 366.
16. T. T. Qin, J. Li, H. Q. Luo, *Corrosion Science*, 53(2011)1072.
17. R. Solmaz, E. A. Şahin, A. Döner, *Corrosion Science*, 53(2011)3231.
18. X. Zheng, S. Zhang, W. Li, *Corrosion Science*, 80(2014)383.
19. X. H. Zhang, Q. Q. Liao, K. B. Nie, *Corrosion Science*, 93(2015)201.
20. E.S. Ferreira, C. Giancomelli, F.C. Giacomelli, A. Spinelli, *Materials Chemistry & Physics*, 83(2004)129.
21. W. H. Li, Q. He, S. T. Zhang, *Journal of Applied Electrochemistry*, 38(2008)289.
22. Y. Ying, W. Li, L. Cai, *Electrochimica Acta*, 53(2008)5953.
23. M. A. Elmorsi, A. M. Hassanein, *Corrosion Science*, 41(1999)2337.

24. G. Quartarone, M. Battilana, L. Bonaldo, T. Tortato, *Corrosion Science*, 50 (2008) 3467.
25. Y. Qiang, S. Zhang, S. Xu, *Journal of Colloid & Interface Science*, 472(2016)52.
26. S. Hong, W. Chen, Y. Zhang, *Corrosion Science*, 66(2013)308.
27. R. Solmaz, G. Kardaş, M. Çulha, *Electrochimica Acta*, 53(2008)5941.
28. N. D. Nam, V. Q. Thang, N. T. Hoai, *Corrosion Science*, 112(2016)451.
29. Y. Qiang, S. Zhang, L. Guo, *Journal of Cleaner Production*, 152(2017)17.
30. D. Wang, B. Xiang, Y. Liang, *Corrosion Science*, 85(2014)77.
31. X. Ma, X. Jiang, S. Xia, *Applied Surface Science*, 371(2016)248.
32. Matjaž Finšgar, Darja Kek Merl, *Corrosion Science*, 83(2014)164.
33. N. Labjar, M. Lebrini, F. Bentiss, *Materials Chemistry & Physics*, 119(2010)330.
34. X. Zhou, H. Yang, F. Wang, *Electrochimica Acta*, 56(2011)4268.
35. W. Chen, H. Q. Luo, N. B. Li, *Corrosion Science*, 53(2011)3356.
36. K. F. Khaled, *Corrosion Science*, 52(2010)3225.
37. Yilmaz N, Fitoz A, Ümit Ergun, *Corrosion Science*, 111(2016)110.
38. G. Gece, *Corrosion Science*, 50(2008)2981.
39. F. Zhang, Y. Tang, Z. Cao, *Corrosion Science*, 61(2012)1.
40. I. B. Obot, N. O. Obi-Egbedi, E. E. Ebenso, *Research on Chemical Intermediates*, 39(2013)1927.
41. O. Benali, L. Larabi, M. Traisnel, *Applied Surface Science*, 253(2007)6130.
42. M. Yadav, D. Behera, S. Kumar, *Industrial & Engineering Chemistry Research*, 52(2013)6318.
43. N. O. Obi-Egbedi, I. B. Obot, *Corrosion Science*, 53(2011)263.
44. X. Li, S. Deng, H. Fu, *Electrochimica Acta*, 54(2009)4089.
45. D. Zhang, Y. Tang, S. Qi, *Corrosion Science*, 102(2016)517.
46. A. Döner, A. O. Yüce, G. Kardaş, *Industrial & Engineering Chemistry Research*, 52(2013)9709.
47. S. H. Kumar, S. Karthikeyan, *Industrial & Engineering Chemistry Research*, 52(2013)7457.
48. P. M. Krishnegowda, V. T. Venkatesha, P. K. M. Krishnegowda, *Industrial & Engineering Chemistry Research*, 52(2013)722.
49. N. Labjar, M. Lebrini, F. Bentiss, *Materials Chemistry & Physics*, 119(2010)330.
50. A. Y. Musa, A. A. H. Kadhum, A. B. Mohamad, *Corrosion Science*, 52(2010)3331.
51. N. O. Obi-Egbedi, I. B. Obot, *Corrosion Science*, 53(2011)263.
52. V. R. Saliyan, A. V. Adhikari, *Corrosion Science*, 50(2008)55.
53. A. K. Singh, M. A. Quraishi, *Corrosion Science*, 52(2010)1373.
54. N. Soltani, M. Behpour, S. M. Ghoreishi, *Corrosion Science*, 52(2010)1351.
55. A. Yousefi, S. Javadian, J. Neshati, *Ind.eng.chem.res*, 53(2014)5475.
56. A. Y. Musa, A. B. Mohamad, A. A. H. Kadhum, *Corrosion Science*, 53(2011)3672.
57. A. Y. Musa, A. A. H. Kadhum, A. B. Mohamad, *Corrosion Science*, 52(2010)526.
58. P. Lowmunkhong, D. Ungthararak, P. Sutthivaiyakit, *Corrosion Science*, 52(2010)30.
59. B. Tan, S. Zhang, Y. Qiang, *Journal of Colloid and Interface Science*, 526(2018)268.